

Surveying the Weather from NOAA's Arc Through the Lens of Network Science

Margherita Kyna Amanda A. Baluyut, Joaquin Emmanuel J. Gonzales,
Geriandre M. Piquero, Bonnie Jenniedy J. Ruiz

Abstract—Through this project, we constructed and analyzed global climate networks from spatio-temporal datasets, with the goal of uncovering climate patterns in terms of underlying network structure. We were able to represent the climate patterns spanning the past eight decades (1950-2020) through networks, with National Oceanic and Atmospheric Administration (NOAA) climate stations as nodes and their maximum temperature correlations as edges. Applying community detection algorithms identified temperature-related locations, even those that are continents and kilometers apart. Employing centrality-based measurements revealed the network's highly central locations, which were determined to be the most vulnerable and at-risk to climate change hazards. Implementing machine learning models supplemented this effort as we were able to utilize network statistics as features in predicting the vulnerability of locations to the impacts of climate change, with significant accuracy, precision, and recall.

Keywords—climate patterns, climate change, climate network, network science, machine learning

I. INTRODUCTION

It has been said that our generation is the first to feel the sting of climate change, and the last that can do something about it.[1] As the effects of global warming worsen each year, governments across the globe have been reorienting their initiatives toward addressing the root causes of climate change and minimizing its impact on vulnerable communities.[2][3] In 2021, the governments of the United States and Canada created the Greening Government Initiative, a community of practice with the objective of engaging governments across the globe in more environmentally sustainable operations.[4] The forum was designed to foster international collaboration between governments and provide a platform for knowledge-sharing and innovation regarding climate issues and effective policies. This is not the only case of countries joining forces to accelerate climate action, and there are numerous global coalitions with similar environmental advocacies such as The Paris Agreement, Climate & Clean Air Coalition, and Alliances for Climate Action, to name a few.[5][6][7]

Due to the interrelated nature of these types of endeavors, network science can play an important role in accelerating these collaborative efforts. There have been many studies that explored the use of network science in the field of climate studies. In 2003, Tsonis and Roeber explored the architecture of the climate network using wind flow data collected across 2,664 points around the world. They were able to find that the earth's climate network exhibited small-world properties, which explained two characteristics of the network: its ability to efficiently propagate fluctuations from one point to another and its ability to maintain stability. They found two distinct subnetworks: a fully connected network within the tropics and a scale-free network at higher latitudes.[8]

In other research, a climate network was constructed with observation sites across the world as nodes, and edges that represent a correlation between a given parameter measured in two connected sites. The study prescribed connecting two nodes if data collected at each observation site exhibited synchronous extreme behavior within a 3 to 7-day window, and if this behavior happened significantly often. Using this structure, strong rainfall was analyzed to find teleconnections, or climate anomalies occurring between points at large distances from each other.[9]

A 2010 work by Steinhaeuser et al. used variables related to surface and atmospheric climate to construct a network with nodes and edges similar to that used in the previously noted study. In their research, the earth was represented as a spatiotemporal grid, with each grid cell corresponding to one node. Absolute values of the correlation coefficient were also used as it considers an inverse relationship between areas as relevant. Similar to other studies, network pruning was done by thresholding the correlation coefficient. A predictive model was created by using derived predictors from extracted clusters to predict air temperature and precipitation. The study concluded that prediction using network-based clusters performed significantly better than when using traditional clustering methods.[10]

This study aims to use network science to explore the interrelated nature of the climate crisis from a different angle. We do this by studying the connection between global locations with the objective of identifying similar countries that may engage in collaborative environmental efforts together, motivated by the fact that their climates are related with each other. The maximum temperature of various areas around the world can be used to map out correlated points in order to form a climate network. We can then identify locations highly correlated with each other using community detection, compare the evolution of communities spanning several decades, and determine vulnerable countries that may be at-risk to hazards brought about by climate change. A machine learning model can also be built using the centrality measures and network statistics to predict whether an area is susceptible to climate change effects due to high levels of precipitation.

II. DATA DESCRIPTION

The data was sourced from the Global Historical Climatology Network Daily (GHCND) dataset from the National Oceanic and Atmospheric Administration (NOAA) through Google BigQuery. There are two datasets extracted: (1) daily climate data from land-based measurement stations in 183 countries, and (2) stations data that includes the names and coordinates of the climate stations worldwide. The *Element* field of the climate data contains the meteorological measurements recorded at the time of observation: (1) TMAX or the maximum temperature, (2) TMIN or the minimum temperature, (3) TAVG or the average temperature, and (4) PRCP or precipitation.[11] The first three temperature elements

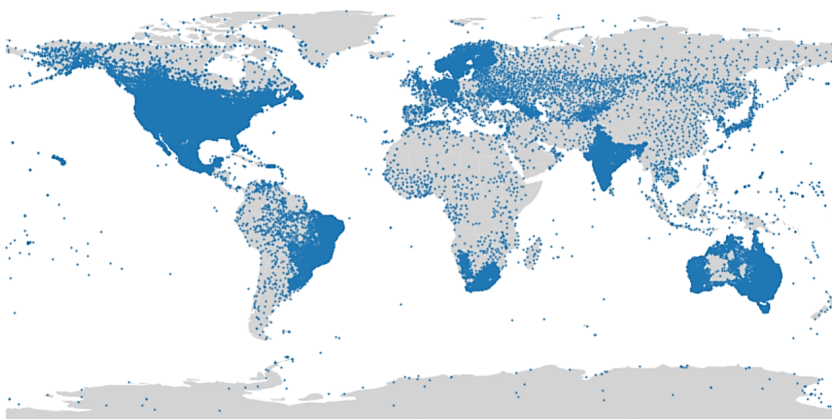


Figure 1. The world map is overlaid with NOAA climate stations represented by the blue dots. The solid blue areas represent stations that are clumped together.

were utilized to identify the threshold that defines the connection between nodes, while only TMAX was used to construct the climate networks. We determined TMAX as the appropriate metric for capturing extreme climatic occurrences in the networks, whereas PRCP as the appropriate target variable for predicting the vulnerability of an area to climate change impacts.

III. METHODOLOGY

This project involved five major processes:

A. Nodes Pruning

In order to build the climate networks, the nodes and edges should be defined. The NOAA datasets consist of about 200,000 climate stations worldwide and creating a network with this many nodes poses efficiency and performance challenges.

As shown in Figure 1, the nodes are extremely close to one another, which may result in redundant nodes and bloated edges when computed and plotted. We employed a filtering of correlations method that helped us achieve a network with evenly distributed nodes. Following the structure suggestions from previous studies on climate patterns [12], we included only one station per grid. The stations were sorted based on the frequency of their TMAX observations. A station is removed if it exists within two units relative to its neighboring stations. An illustration is shown in Figure 2.

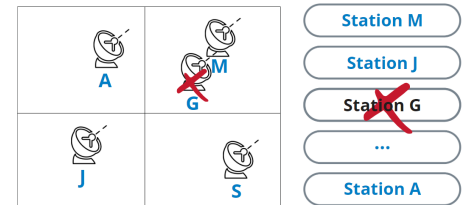


Figure 2. An illustration of how the filtering method was done. Station G was removed because it exists in the same grid as station M.

We employed a filtering of correlations method that helped us achieve a network with evenly distributed nodes. Following the structure suggestions from previous studies on climate patterns [12], there would be no two stations that are geographically close to each other. This is also implemented to avoid spatial autocorrelation. The stations were sorted based on the

frequency of their TMAX observations. A station is removed if it exists within two units relative to its neighboring stations. An illustration of how this was performed is shown in Figure 2, while the resulting map of nodes for climate network construction is shown in Figure 3.



Figure 3. The resulting map of the climate stations that will serve as network nodes. Stations that are close to other stations and have fewer observations were pruned to avoid spatial autocorrelation.

B. Calculation of Correlations and Selection of Cutoff Value

We used the temperature elements (TMIN, TAVG, and TMAX) to get the edge values by calculating the Pearson correlation coefficient ρ for each pair of climate stations i and j , given by

$$\rho_{i,j} = \frac{\text{cov}(i, j)}{\sigma_i \sigma_j}$$

where we generated correlation matrices with values ranging from -1 to 1. A value close to 1 implies that as the temperature of station i rises or falls, the temperature of station j tends to follow the same trend; a value close to -1 suggests the opposite.

Using the correlation matrix, we created the adjacency matrix A defined as:

$$A_{ij} = \begin{cases} 0 & \text{if } \rho_{ij} < \delta \\ 1 & \text{if } \rho_{ij} \geq \delta \end{cases}$$

where the threshold δ determines the presence or absence of the connectivity of two stations.

To define the relationship between each node, we first simulated various correlation thresholds per element type per year. For all three elements, 0.9 exhibits a power-law distribution, which is a property of scale-free networks, and was thus chosen as the cutoff. Figure 4 illustrates the simulations for the year 2020 using TMAX.

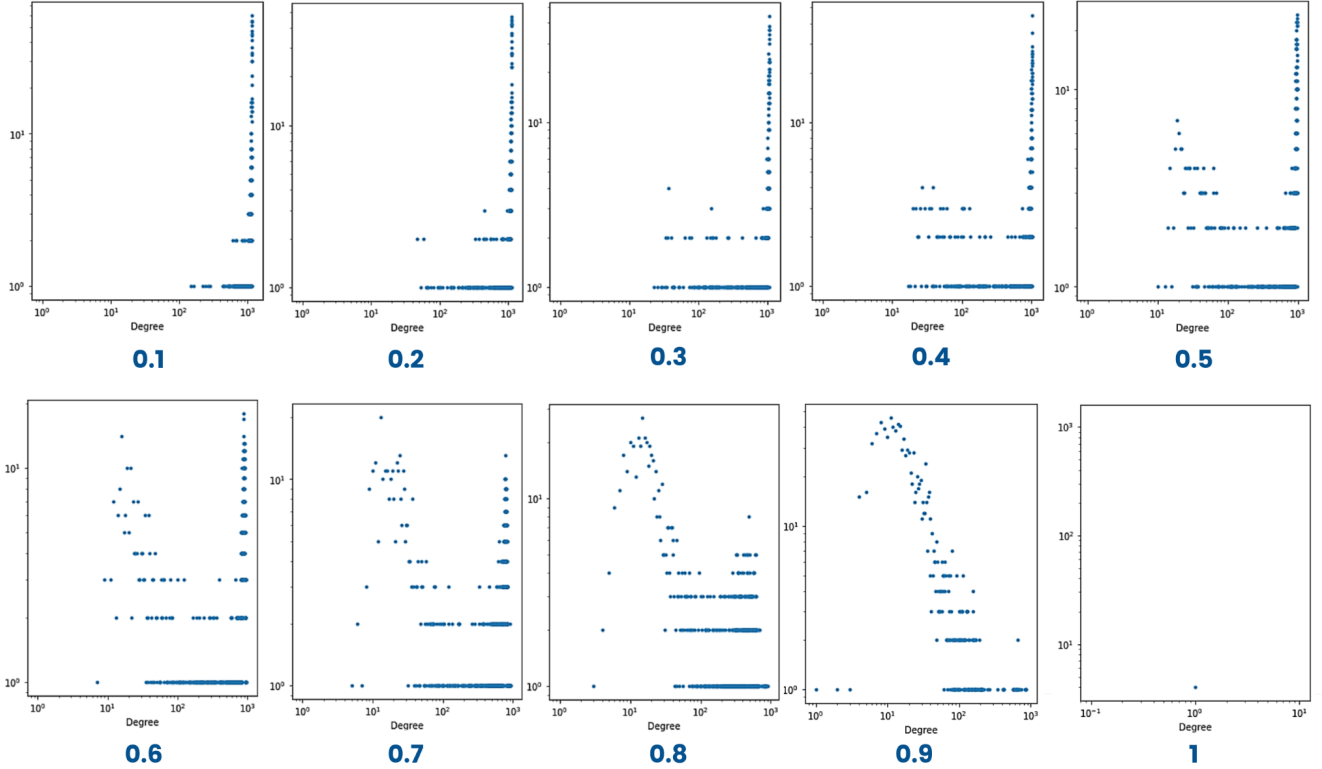


Figure 4. The distributions of the maximum temperature correlations between climate stations per cutoff value for the year 2020. The 0.9 was chosen as the threshold that defines a connection between a pair of nodes because it follows a power-law distribution.

C. Network Construction

We created weighted, undirected, and disconnected networks for all available years (1950, 1960, 1970, 1980, 1990, 2000, 2010, 2020) with climate stations as the nodes and TMAX correlation greater than 0.9 as the edge. In addition, we also considered a pair of nodes with a high negative correlation as connected since there are climate oscillations we wanted to capture. The network properties of the eight constructed global climate networks are shown in Table 1.

D. Network Analysis

We utilized the agglomerative approach Louvain algorithm, which uses modularity M_c to detect communities and quantify their strengths in the networks. It is given by

$$M_c = \sum_{c=1}^{n_c} \left[\frac{L_c}{L} - \left(\frac{k_c}{2L} \right)^2 \right]$$

where n_c is the number of communities, L_c is the number of links inside the community, k_c is the total degree of nodes in the community, and L is the total number of links in a particular network.[13]

Table 1. Network properties of the global climate networks for the years covered in this project. The topological parameters vary per decade, with observed significant changes in the 1990s.

Year of Observation	Nodes	Edges	Ave. Clustering
1950	711	8,496	0.45
1960	1,021	16,250	0.48
1970	978	16,955	0.45
1980	1,304	23,083	0.38
1990	1,348	33,040	0.34
2000	1,330	28,978	0.40
2010	1,268	21,603	0.42
2020	1,204	27,876	0.41

Centrality measures indicate how influential or significant a node is within the overall network. We

discovered that closeness centrality provided no additional value to the created climate networks, thus we limited our analysis to (1) degree centrality, (2) betweenness centrality, and (3) eigenvector centrality.

The degree centrality of a climate station i represents the number of stations connected to it in comparison to the total number of stations in the network to which it may possibly connect to ($n - 1$), which translates to the significance of climate station i within its local environment, and given by

$$D(i) = \frac{1}{n-1} \sum_{j=1}^n A_{ij},$$

where A_{ij} is the ij^{th} element of the adjacency matrix A of the network.[14]

The betweenness centrality as a global topological measure estimates how frequently paths in the network include climate station i , quantifying its role as a connector to other stations, and given by

$$C_B(v) = \sum \frac{\sigma_{ij}(v)}{\sigma_{ij}}$$

where σ_{ij} is the total number of shortest paths from station i and station j , and $\sigma_{ij}(v)$ is the number of shortest paths passing through station v .[14]

Finally, the eigenvector centrality x was used to calculate the value of climate station v based on its important connections, and given by

$$x_v = \frac{1}{\lambda} \sum_{t \in G} a_{v,t} x_t$$

where G is the number of other nodes in the network, $a_{v,t}$ is the value in the adjacency matrix corresponding to station v and station t , x_t is the eigenvector centrality of station t , and λ is the eigenvalue of the adjacency matrix.[15]

D. Machine Learning Model

Machine learning classification models were built to predict whether an area is vulnerable to climate change due to high levels of precipitation. In this exercise, precipitation was the target variable, with all four centrality measures and the average clustering coefficients as features. Following the computation of

the baseline, we implemented four models: Logistic Regression, Decision Tree, Random Forest, and Gradient Boosting Method. The SHAP interpretability method was then applied to the best model to extract the important feature/s that influenced the model's prediction.

IV. DISCUSSION OF RESULTS

A. Global Climate Network of 2020

From our analysis, we have found that the network exhibits teleconnection, which is spatial patterns in the atmosphere that link weather and climate anomalies over large distances across the globe. These relationships can be detected in a network through community methods such as the Louvain algorithm.[16] Through this method, five communities were identified and displayed in Figure 5.

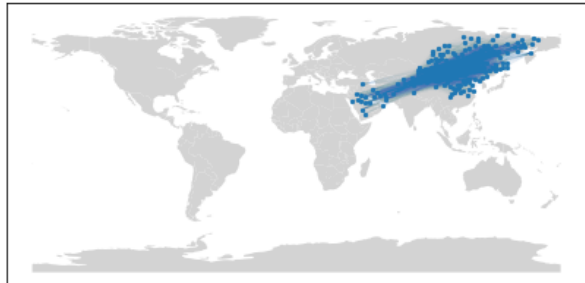
One community was the Saudi-China-Northeast Asia network. It is worth noting that Saudi Arabia and China are known to be strategic allies, which could be the reason this community was identified. [17]

Another was the Southern Hemisphere-Russia network, whose climates are not similar but may still be related to one another.[18]

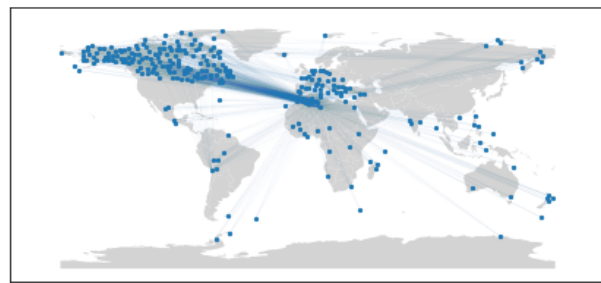
The Central Asia network was also identified, which contains countries located very near each other.

We also observed a Canada-Southern Europe network, where countries are separated by an ocean between them.

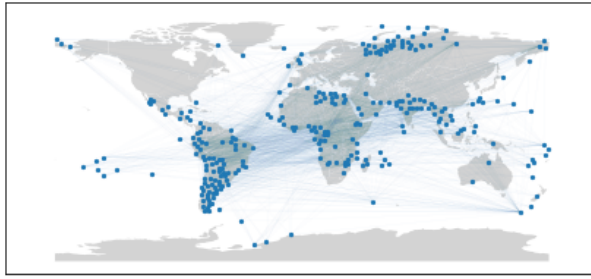
Finally, the last and largest identified community was a network deduced to reflect the impact of industrialization and climate change. In this network, we notice that developed countries such as the US, South Africa, China, and Australia are part of the community of a station located in Antarctica. This relationship may reflect the effects of melting ice caps at the poles due to the greenhouse effect contributing to changing weather patterns around the globe.[19]



(1) The Saudi Arabia-China-North East Asia Climate Network



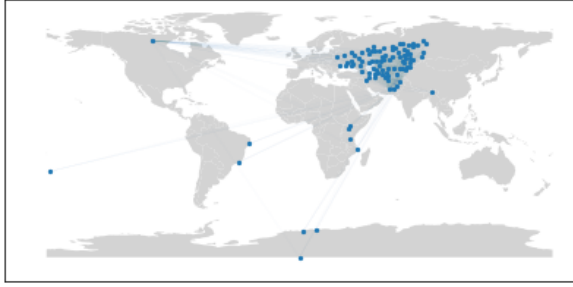
(2) The North America and Europe Climate Network



(3) Russia-Southern Hemisphere Network



(4) The Impact of Industrialization Climate Network (US-Australia-Europe-Antarctica)



(5) Central Asia Climate Network

Figure 5. Using the Louvain method on the global climate network of 2020, five communities were detected:
 (1) Saudi-China with North-East Asia, (2) Southern Hemisphere-Russia, (3) Central Asia, (4) Canada-Southern Europe,
 and (5) a community that reflects the impact of industrialization and climate change.

An additional insight that we can deduce from these derived communities is that these correlated countries could adopt similar voting conventions and strategies on global climate matters. These countries will benefit by working together because they may have related extreme temperatures and share the same motivation. One of the cases we have identified is the mentioned China and Saudi Arabia relationship where the two countries sought to prevent a UN climate deal in Scotland from including language that opposes fossil fuel subsidies.[20]

B. Largest Communities in the Global Climate Networks per Decade

We proceed to contrast the largest among the resulting communities derived from the Climate Network using 2020 data against the data from 1950, 1960, 1970, 1980, 1990, 2000, and 2010. We would then be able to assess the evolution of the climate network relationships over time. Figure 6 illustrates the geographic properties of nodes and edges in the largest community of each decade, while Table 2 shows their network properties.

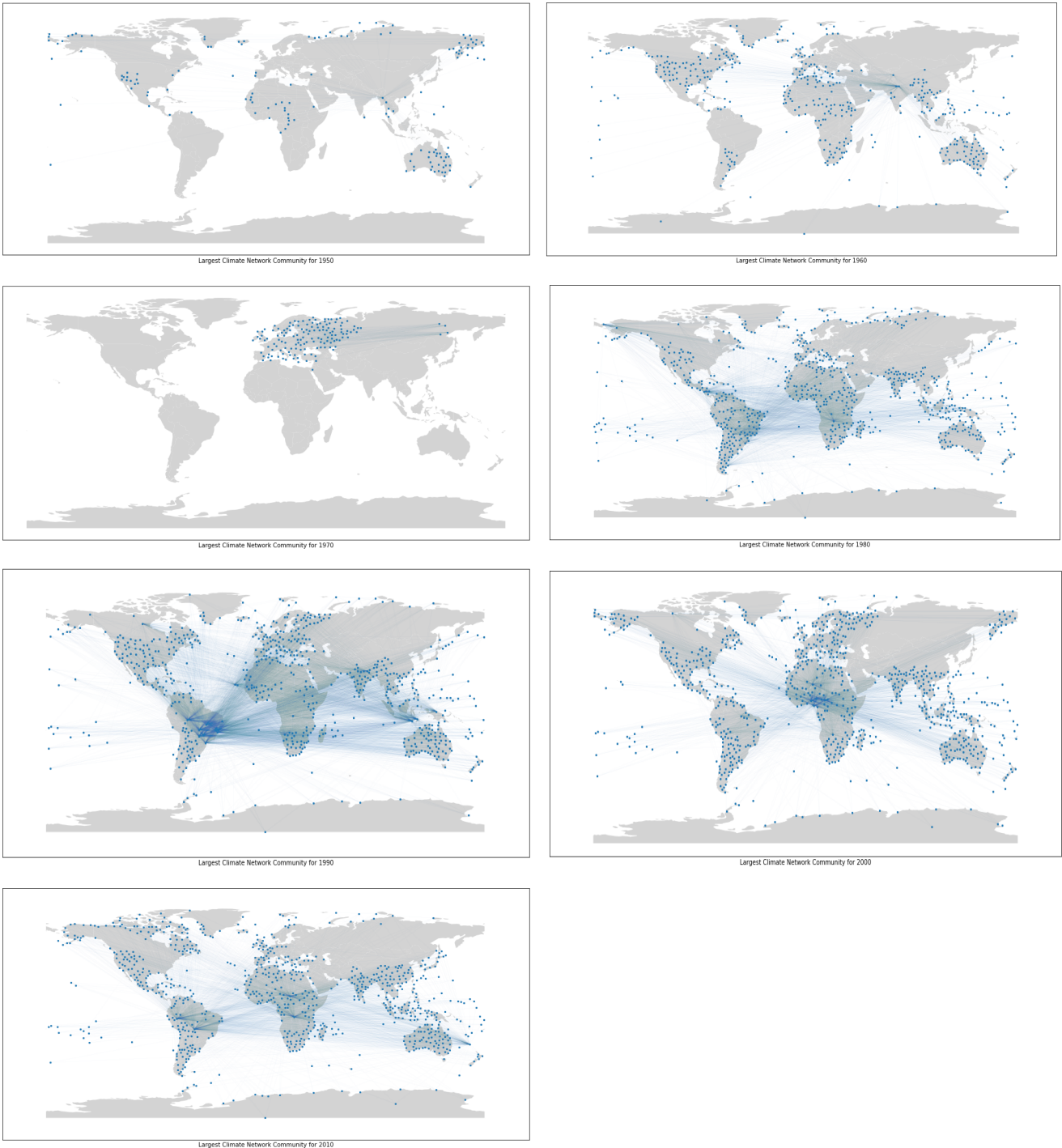


Figure 6. Using the Louvain method on the global climate network for the years included in this study, the resulting top communities for each year are compared. Notice that the resulting top communities for the years 1950, 1960 and 1970 are lesser in magnitude compared to the top detected communities for the years 1980, 1990, 2000 and 2010.

Beginning in the decade of 1950, we see that the largest community identified contained the fewest number of nodes and edges compared to the largest communities of subsequent decades. Additionally, its average clustering coefficient was much larger than in recent years. This implied fewer correlations between areas, and interrelated temperatures belonged within clusters. In the next decade, the largest community

possessed noticeably more nodes and edges and spanned across larger geographic regions. It was found that an environmental crisis happened in the late 1960s, with highly publicized environmental catastrophes involving smog, oil spills, and fires. Researchers started pointing to the exponentially increasing population as the problem, and a number of revelatory books were published on environmental

awareness during this time.[21] In the 1970s, the largest community identified involved Europe and some parts of Russia. Although it contained less nodes than communities in previous decades, a high number of connections between these nodes existed. During this decade, the European Union established the first environment ministries and adopted its first Environment Action Programme. This period was also described as the decade of the environmental movements.[22]

The 1980s showed a drastic increase in the number of nodes and edges in the largest community identified, much larger than any previous decade. There were more connections between nodes at great distances apart in this community, indicating more correlations between distant areas around the world. It also showed a drop in the average clustering coefficient, implying that nodes were less isolated. It was during this time that Europe and North America began experiencing phenomena such as acid rain, resulting in growing concerns about the protection of the ozone layer. The Vienna Convention for the Protection of the Ozone Layer was created in 1985, aiming to reduce the use of chlorofluorocarbons.[23] The trend of increasing edges observed in the largest communities persisted through the 1990s decade—almost double that of the previous

period—accompanied by a further decrease in the average clustering coefficient. More correlations were also observed in areas separated by large distances, where a dense number of edges originating in the African continent reach as far as Europe and Asia. During this time, the second World Climate Conference declared climate change as a global problem that required a global response.[24] The largest community during the decade of 2000 also had the largest number of nodes among all decades, but the number of edges decreased to almost half that of the previous decade. However, there were still connections that spanned large distances, primarily involving the African continent. It was during this time that the Kyoto Protocol entered into force, which was regarded as one of the most influential actions taken in terms of climate change. It aimed to reduce greenhouse gas emissions of industrialized countries from 2008 to 2012.[25]

By the 2010 decade, the largest community still possessed similar characteristics to that of the decade before it. However, by 2020 there was an observable decrease in the number of nodes and edges, along with the average clustering coefficient. This may reflect the improvements in climate policies, initiatives on global collaboration, and overall increased environmental awareness observed in recent years.

Table 2. Network properties of the largest communities identified in the global climate networks for the years covered in this project.

Year of Observation	Largest Community Nodes	% to total	Largest Community Edges	% to total	Largest Community Ave. Clustering
1950	150	21%	279	3%	0.37
1960	429	42%	1,150	7%	0.37
1970	146	15%	1,434	8%	0.62
1980	734	56%	4,411	19%	0.18
1990	691	51%	7,723	23%	0.20
2000	839	63%	4,637	16%	0.25
2010	814	64%	4,112	19%	0.28
2020	384	32%	2,477	9%	0.33

C. Centrality Measures for the Global Climate Network of 2020

Using the Climate Network derived from the 2020 data, we were able to compute the degree centrality,

betweenness centrality, and eigenvector centralities of each node in the network. The most central nodes are highlighted in a darker shade of red color as seen in Figures 7, 8, and 9.

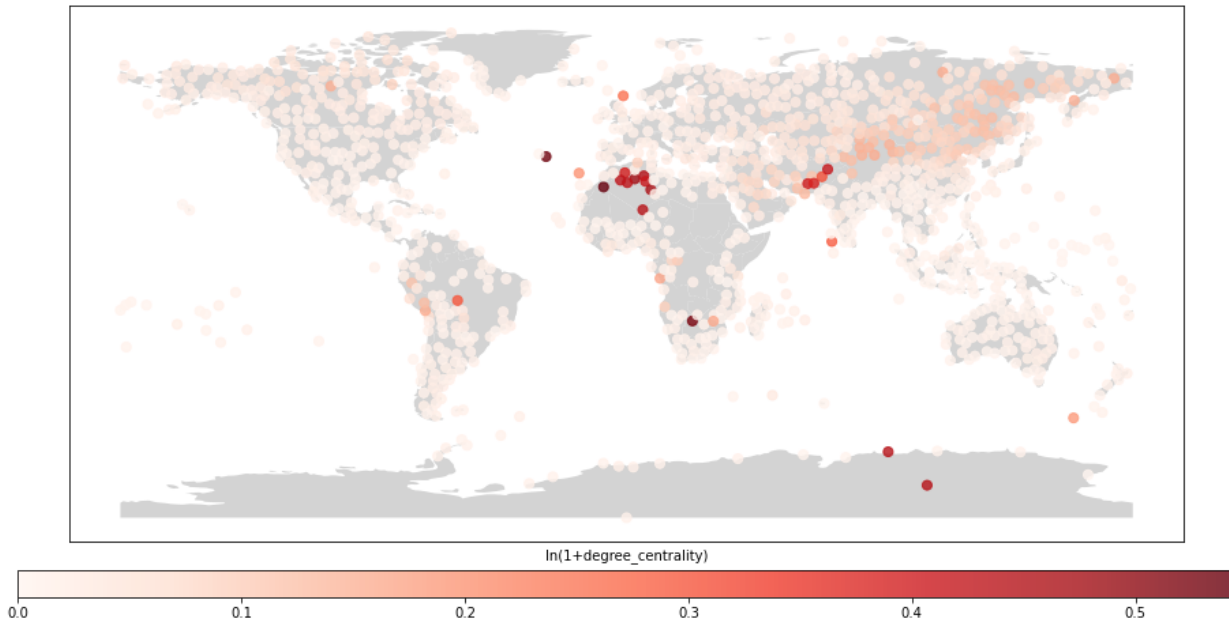


Figure 7. Computing for the degree centrality for each node in the 2020 global climate network. Locations that have relatively high degree centralities are the United Kingdom, Northwest Africa, Pakistan, South Africa, South India, Central South America, and stations in Antarctica. Values are displayed in the natural logarithm scale.

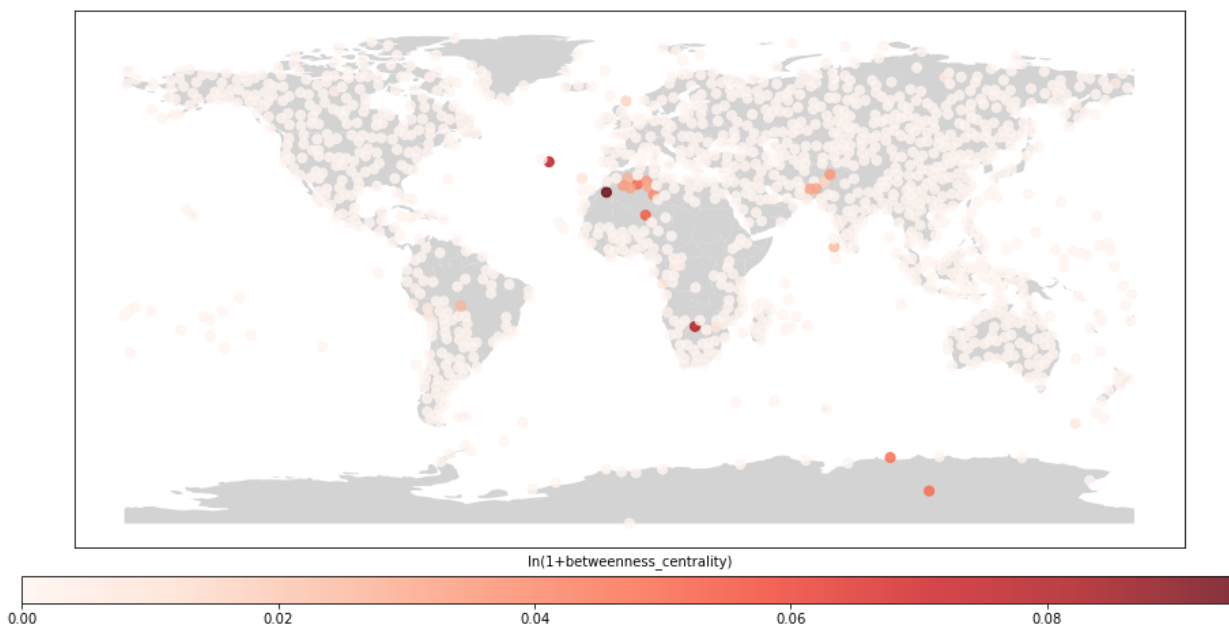


Figure 8. Computing for the betweenness centrality for each node in the 2020 global climate network. Locations that have relatively high betweenness centralities are the North Atlantic Ocean, Northwest Africa, Pakistan, South Africa, South India, and stations in Antarctica. Values are displayed in the natural logarithm scale.

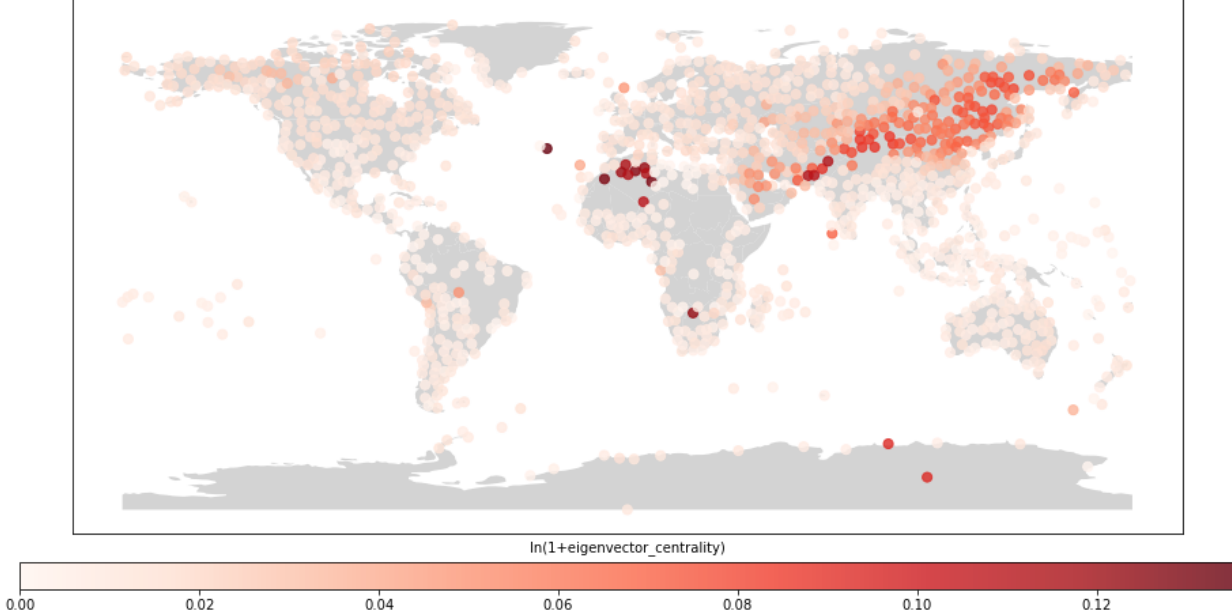


Figure 9. Computing for the eigenvector centrality for each node in the 2020 global climate network. Locations that have relatively high betweenness centralities are the North Atlantic Ocean, Northwest Africa, Pakistan, South Africa, South India, stations in Antarctica, and the countries within the China-Saudi Arabia climate network. Values are displayed in the natural logarithm scale.

Using the three network centrality measures, we identified common locations that are most central relative to others for all three methods. These are Northwest Africa, Southern Africa, Pakistan, South India, and a few locations in Antarctica. Given that these are highly central nodes or locations in the climate network, these are countries that are highly related to or impacted by global climate developments. As such, these locations can be defined as climate vulnerable.

D. Machine Learning Models

Using the centrality measures and the network statistics calculated via the network of weather stations formed by taking the correlation of maximum temperatures during 2020, we wanted to build a model that would help identify areas that are highly susceptible to the effects of climate change. In building the machine learning models, we used the level of precipitation recorded by each weather station as an indicator of climate change effects. Given that one of the major effects of climate change would be high temperatures, we would expect warmer oceans, which translates to faster rates of evaporation. As there is more water vapor concentration in the atmosphere due to more evaporation, it is expected that there would be higher levels of precipitation among areas that are mostly affected by climate change. A study conducted by the World Meteorological Organization indicates that countries

found in Southern Africa including Madagascar, Malawi, and Mozambique have experienced cyclones with record-breaking intensities due to global warming.[26] Given that our climate network was able to identify Southern Africa as one of the most vulnerable countries that are mostly affected by the impact of climate change, we argue that network statistics could serve as features for our machine learning models in identifying areas that are susceptible to climate change.

We identify a site as highly susceptible to the effects of climate change if its precipitation level for the entire year of 2020 goes beyond the median precipitation level of all the weather station sites where precipitation data was collected. In evaluating the performance of our machine learning models, the team used the F1-Score metric which assigns equal importance to the consequence of having false positives and false negatives as predicted by the model. To tune each machine learning model's hyperparameters, the Monte-Carlo Cross Validation method was used.

Out of the five different machine learning models implemented, it was the Random Forest Classifier that generated the best performance on the test set as this model produces a 73% accuracy and a 72% F1-score. The predictive capability of the Random Forest Classifier is higher than the 1.25 x Proportional

Table 3. The results of the five different machine learning models implemented are summarized below. It can be seen that the Random Forest Classifier tends to have the best performance on the test set for both accuracy and F1-score metrics.

	Optimal Hyperparameter	Test Accuracy	Test F1-Score	Test Precision	Test Recall
k-Nearest Neighbors	n_neighbors=7	68.13%	67.23%	69.6%	65.29%
Logistic Regression	C = 0.1	70.21%	70.72%	70.04%	71.47%
Decision Trees	max_features=0.8 max_depth=2	69.19%	70.62%	67.84%	74.91%
Random Forest Classifier	max_features=0.6 max_depth=3	72.71%	72.28%	74.04%	70.74%
Gradient Boosting Classifier	max_features=0.6 max_depth=3	71.06%	71.23%	71.38%	71.18%

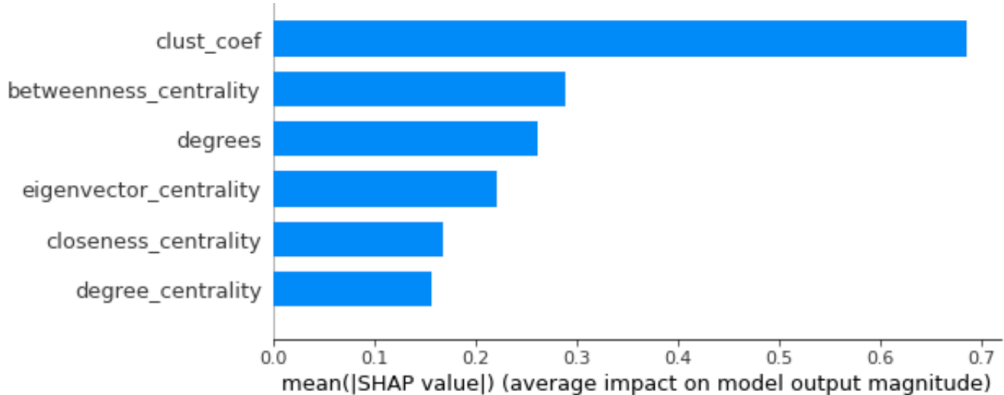


Figure 10. The respective Shapley values of each centrality measure and network statistics were used as features for the top-performing Random Forest Classifier model. The clustering coefficient and the betweenness centrality of each node station are the variables that contribute the most to the model's predictions.

Chance Criterion baseline of 62.5%, which is observed when the model performs a random assignment per observation.

In order to make sense of the best performing Random Forest Classifier, we utilized the SHAP library in order to find the Shapley values or the marginal contribution of each feature to the model's predictions. From the plot above, we observe that the clustering coefficient of each weather station along with their respective betweenness centrality tends to influence the model's predictions as to whether a particular area is strongly affected by climate change effects or not.

V. CONCLUSIONS

Through this project, we were able to leverage Network Science to represent and analyze climate

patterns. Using the maximum temperature correlations and centrality measures, we were able to identify the most vulnerable and at-risk areas to climate change hazards: Northwest Africa, South Africa, Pakistan, South India, and Antarctica. These are the highly central locations to the entire network, implying a close relationship to the drastic changes in temperature and associated consequences.

We also discovered that integrating various network statistics into machine learning models was similarly effective in identifying areas that are potentially vulnerable to impacts of climate change, with the average clustering coefficient and the betweenness centrality being the most influential features. The Random Forest Classifier outperformed the other models and exceeded the baseline accuracy by about 10%, while producing a 72% F1-Score.

VI. FUTURE WORK

Construction of the global climate networks using the three other climate indicators (minimum temperature, average temperature, and precipitation) is recommended to further validate the identified vulnerable and at-risk areas to climate change hazards. Exploring other machine learning models and hyper tuning the parameters are also suggested to optimize the classification results.

VII. REFERENCES

- [1] Cournoyer, Caroline. We're the first generation to feel the sting of climate change. And we're the last who can do something about it. (2019, March 1). *Governing*. <https://www.governing.com/government-quotes/gov-inslee-2020.html>.
- [2] NASA. (2020). World of Change: Global Temperatures. *NASA Official Website; NASA Earth Observatory*. <https://earthobservatory.nasa.gov/world-of-change/global-temperatures>.
- [3] Sisson, Patrick. (2021). The Rise of the Local Climate Candidate. *Bloomberg*. <https://www.bloomberg.com/news/articles/2021-11-23/for-so-me-candidates-climate-change-is-now-a-local-issue>.
- [4] U.S. Department of Energy's Federal Energy Management Program. (2021). Greening Government Initiative. *Office of the Federal Chief Sustainability Officer Official Website*. <https://www.sustainability.gov/ggi/>.
- [5] United Nations. (2015). The Paris Agreement. *United Nations Framework Convention on Climate Change; United Nations*. <https://unfccc.int/process-and-meetings/the-paris-agreement/the-paris-agreement>.
- [6] Environment, U. N. (2017, September 15). Climate and clean air coalition. *UNEP - UN Environment Programme*. <https://www.unep.org/explore-topics/climate-action/what-we-do/climate-and-clean-air-Coalition>.
- [7] Alliances for Climate Action Organization. (2021). Alliances for Climate Action. <https://www.alliancesforclimateaction.org/>.
- [8] Tsonis, A.A., Roebber, P.J. (2003). The architecture of the climate network. *Physica A*. <http://rainbow.ideo.columbia.edu/~alexeyk/Papers/TsonisRoebber2004.pdf>.
- [9] Kurthd, Jurgen. (2022). Climate Meets Network Science. *NetSci Conference 2022*. <https://www.youtube.com/watch?v=DrGn7-j75wU>.
- [10] Steinhaeuser, K. et. al. (2010). Complex Networks as a Unified Framework for Descriptive Analysis and Predictive Modeling in Climate Science. *Wiley Online Library*. <https://onlinelibrary.wiley.com/doi/abs/10.1002/sam.10100>.
- [11] Flamig, Zac. (2021). NOAA Global Historical Climatology Network Daily (GHCN-D). *GitHub*. <https://github.com/awslabs/open-data-docs/tree/main/docs/noaa/noaa-ghcn>.
- [12] Ludeschera, J., et. al. (2020). Network-based forecasting of climate phenomena. Perspective. <https://www.pnas.org/doi/pdf/10.1073/pnas.1922872118>.
- [13] Legara, Erika Fille, T. (2021). Network-Science-Lectures/Community Detection Jupyter Notebook *GitHub*. <https://github.com/eflegara/Network-Science-Lectures/blob/master/Community%20Detection.ipynb>.
- [14] Srinivasan, S., et. al. (2020). Chapter Three - Machine learning techniques for fractured media. *Advances in Geophysics*, Elsevier. <https://doi.org/10.1016/bs.agph.2020.08.001>.
- [15] Ibid.
- [16] Minogue, Paul. (2020). Using network analysis and eigenvector centrality to identify Arsenal's most influential invincibles. *Technological University Dublin*. <https://paulminogue.com/posts/8cdb1f03-f215-4060-908f-d21d403bf9e5>.

- [17] Niyogi, Acacia. (2022). The Future Of Chinese-Saudi Relations. *The Organization for World Peace*. <https://theowp.org/reports/the-future-of-chinese-saudi-relations/>.
- [18] National Geographic Society. (2022). All About Climate. *National Geographic*. <https://education.nationalgeographic.org/resource/all-about-climate>.
- [19] US Department of Commerce, N. O. and A. A. (n.d.). How does sea ice affect global climate? *National Ocean Service*. <https://oceanservice.noaa.gov/facts/sea-ice-climate.html>
- [20] Abnett, K., Piper, E. (2021). China, Saudi seek to block anti-fossil fuel language in UN climate deal –sources. *Reuters*. <https://www.reuters.com/business/cop/china-saudi-seek-block-anti-fossil-fuel-language-un-climate-deal-sources-2021-11-12/>.
- [21] University of Michigan History Department. (2014). “Environmental Crisis” in the Late 1960s. *Exhibit · Give Earth a Chance: Environmental Activism in Michigan*. <http://michiganintheworld.history.lsa.umich.edu/environmentalism/exhibits/show/>.
- [22] European Environment Agency. (2011). 1970s. European Environment Agency Official Website. <https://www.eea.europa.eu/environmental-time-line/1970s>.
- [23] Jackson, Peter. (2022). From Stockholm to Kyoto: a Brief History of Climate Change. *United Nations Official Website*. <https://www.un.org/en/chronicle/article/stockholm-kyoto-brief-history-climate-change>.
- [24] Ibid.
- [24] Ibid.
- [26] World Meteorological Organization. (2022). Climate change increased extreme rainfall in Southeast Africa storms. *World Meteorological Organization Official Website*. <https://public.wmo.int/en/media/news/climate-change-increased-extreme-rainfall-southeast-africa-storms>.
- [27] Waggoner, Ben M. (2009). The Holocene Epoch. *University of California Museum of Paleontology*. <https://ucmp.berkeley.edu/quaternary/holocene.php#>.
- [28] American Institute of Physics. (2021). The Discovery of Global Warming. *Center for History of Physics of the American Institute of PhysicsThe Discovery of Global Warming*. <https://history.aip.org/climate/timeline.htm>.
- [29] Marshall, Michael. (2006). Timeline: Climate Change. *New Scientist*. <https://www.newscientist.com/article/dn9912-timeline-climate-change/>.

VIII. APPENDIX

This section contains the global climate networks constructed per decade.

A. Global Climate Network of 1950

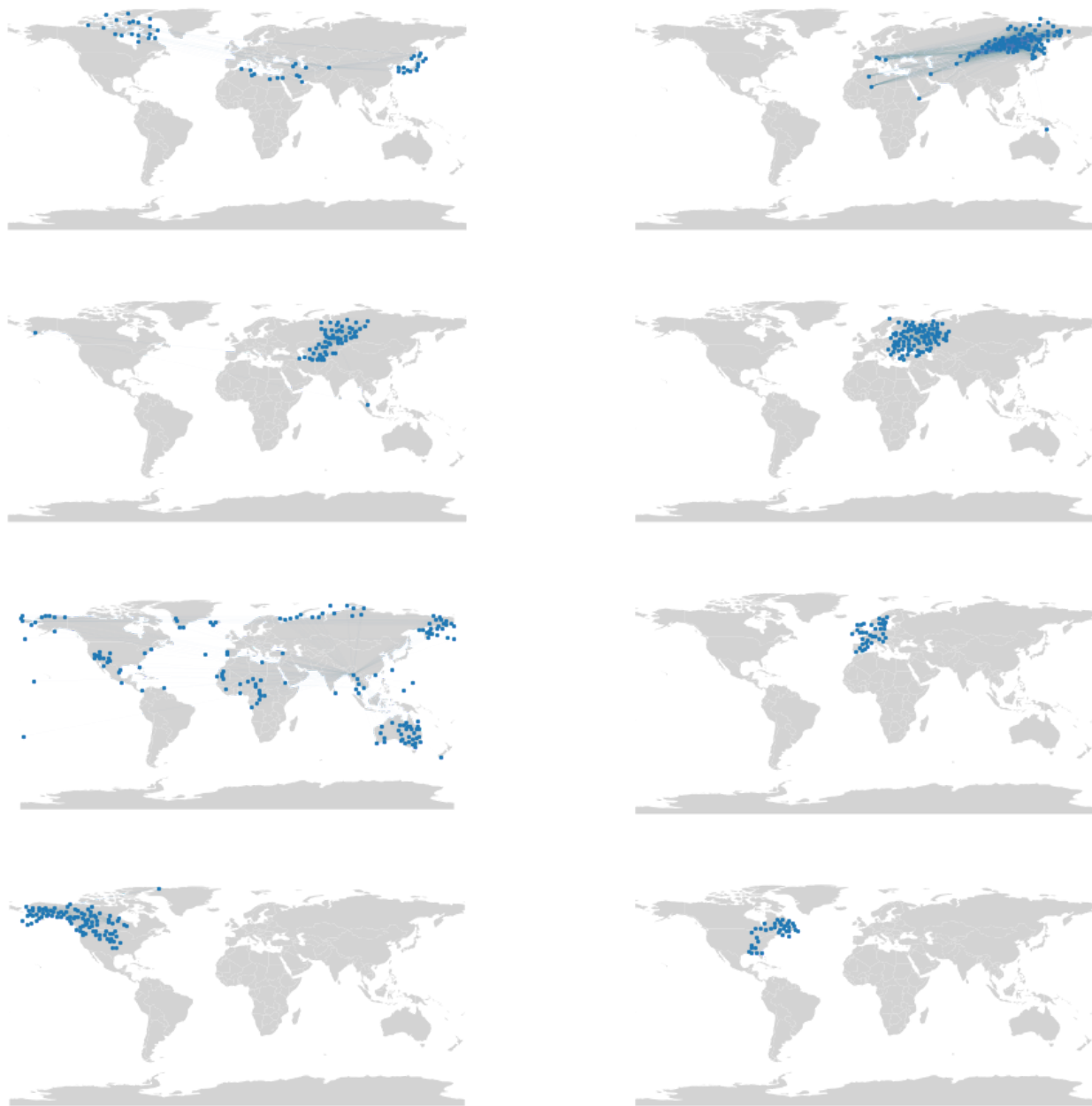


Figure 11. The global climate network of 1950 has the fewest number of nodes (711) and edges (8,496). Smaller, simpler, and more compact climate communities were detected from the network, as depicted in Figure 5. This period was considered the beginning of the Holocene Epoch, with only small-scale climate shifts recorded.[27]

B. *Global Climate Network of 1960*

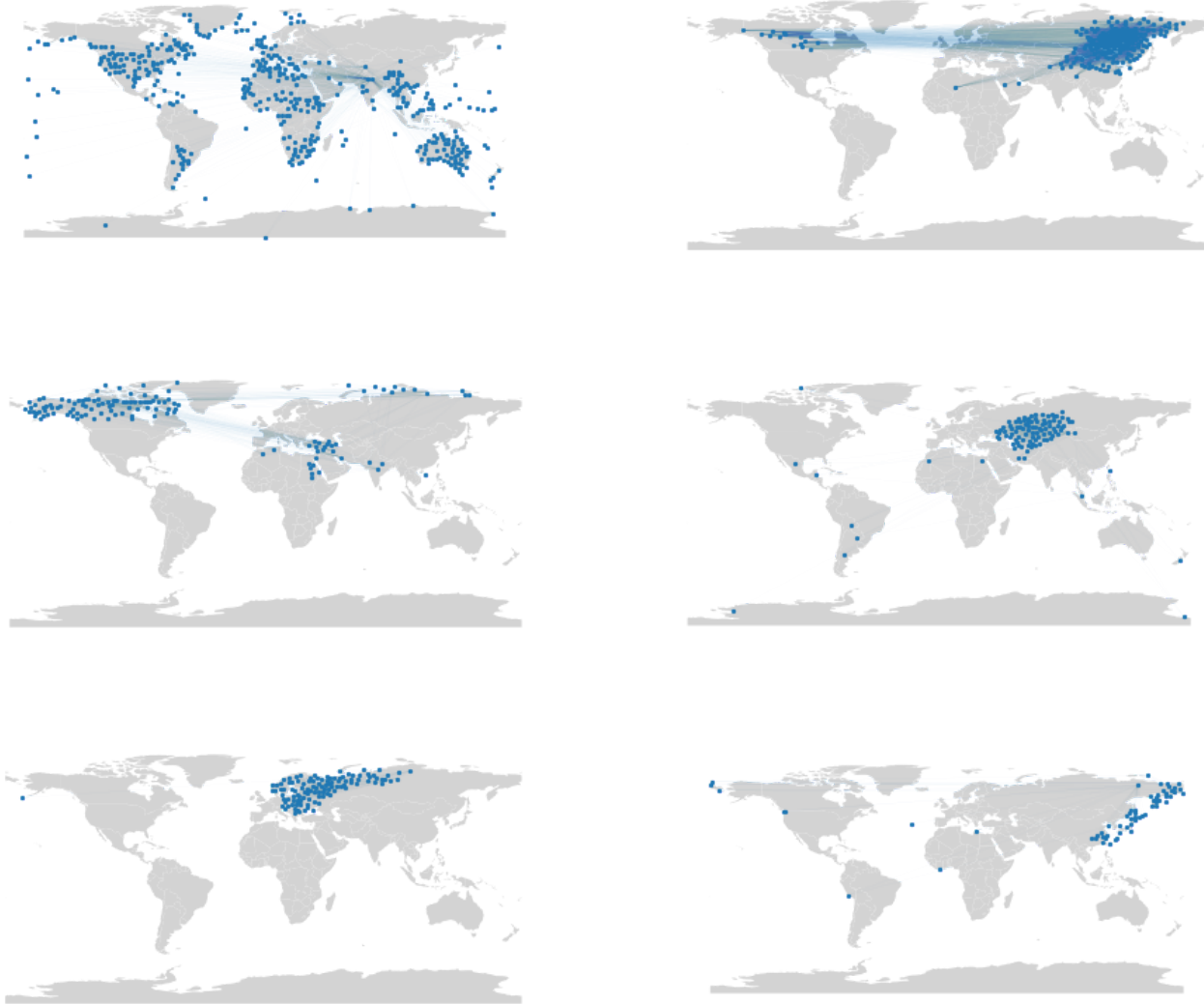


Figure 12. The global climate network of 1960 appears similar to the 1950's which detected small and simple communities. It is also observed that more nodes (1,021) arose and the edges doubled (16,250), yet the increase in the average clustering coefficient is minor (7%). This implies that the increase in the network's size did not lead to a significant increase in connections. Although it is worth noting that during this period, a downturn in global temperatures was recorded.[28]

C. Global Climate Network of 1970

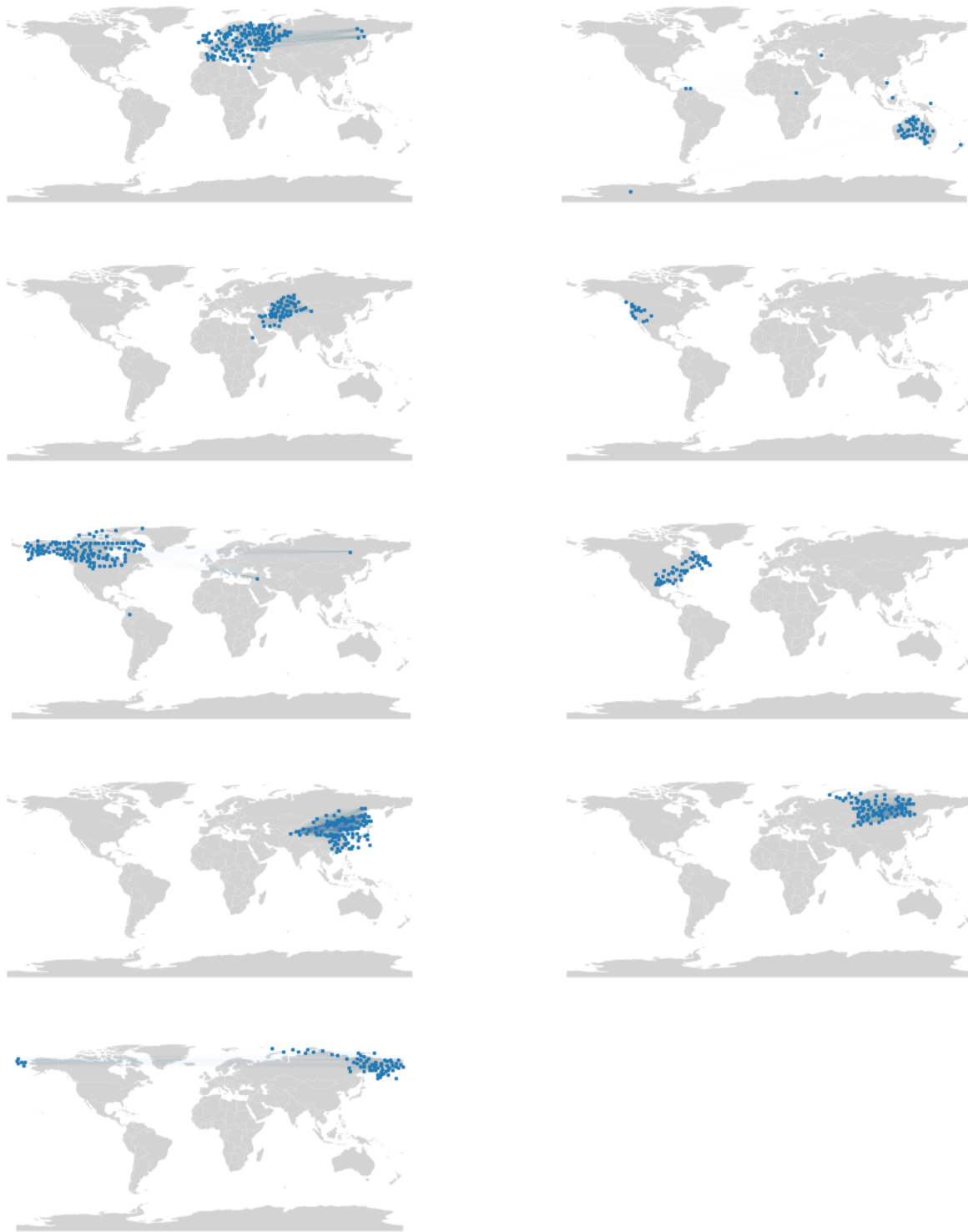


Figure 13. The global climate network of 1970 tends to be more similar to the 1950's than to the preceding decade. The nodes (978) decreased, while the edges remained relatively the same (16,955). This implies that the remaining climate stations established more connections.

D. Global Climate Network of 1980

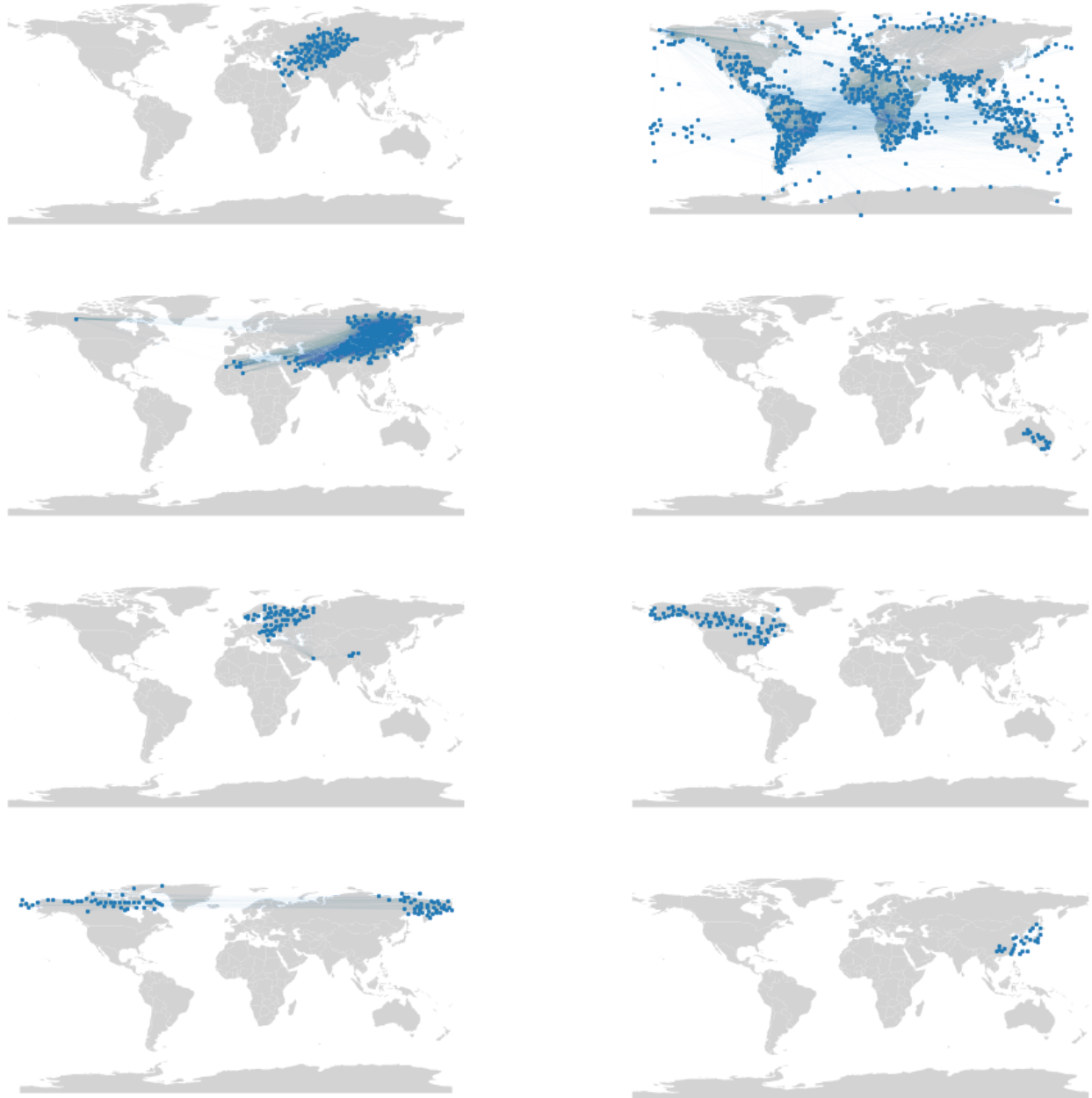


Figure 14. A significant increase in the nodes (1,304) and edges (23,083) was seen in the global climate network of 1980, despite the considerable decrease in the average clustering coefficient (less 15%).

E. Global Climate Network of 1990

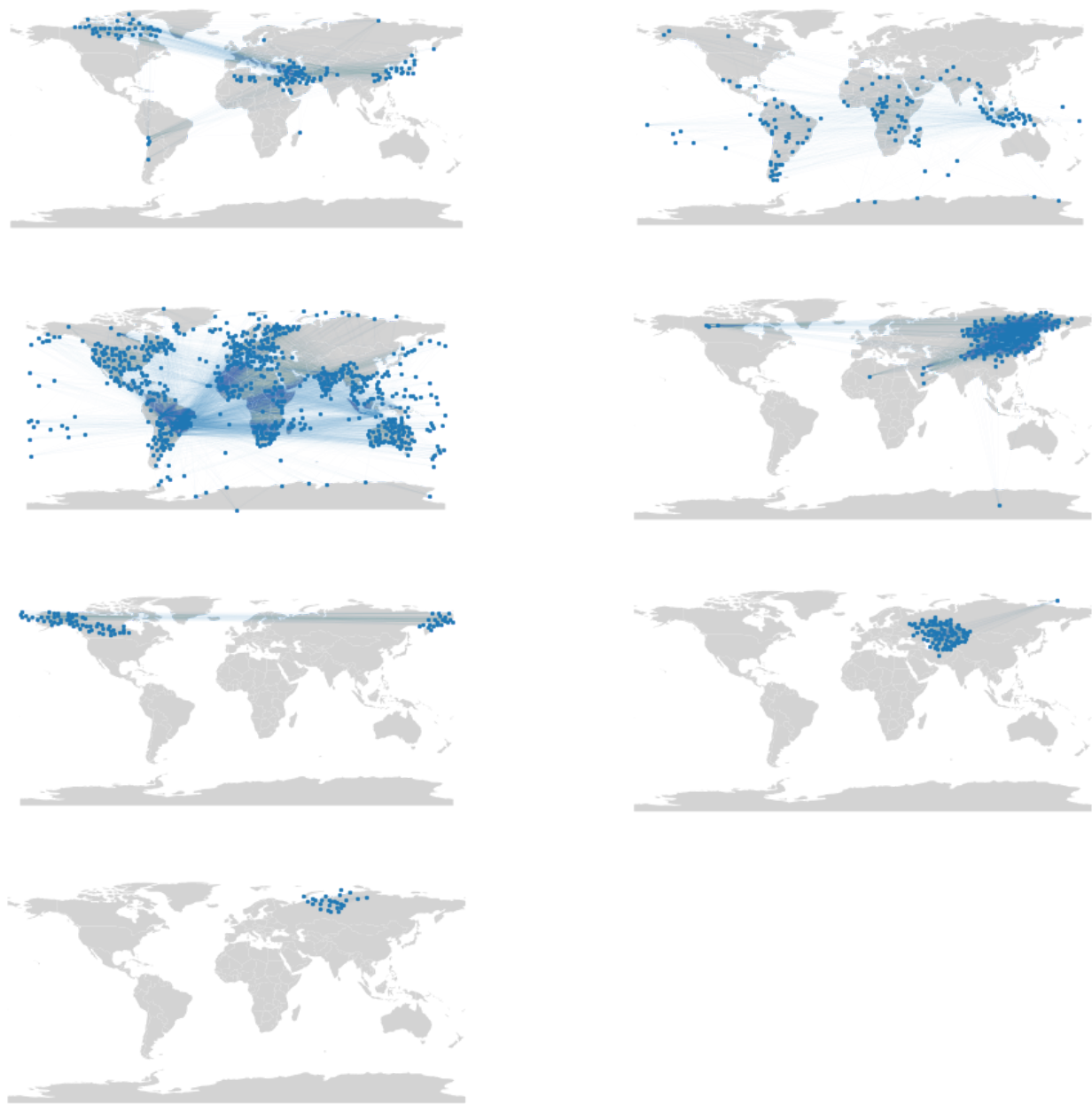


Figure 15. In the global climate network of 1990, the number of nodes remained the same (1,348), but the edges increased by 43%. This may be attributed to the recorded deviations from the global average surface temperature. During this period there were noticeable climate communities that began to span the entire world, pointing to the compounding effects of climate change on even distant countries, and prompting global intervention.[29]

F. Global Climate Network of 2000

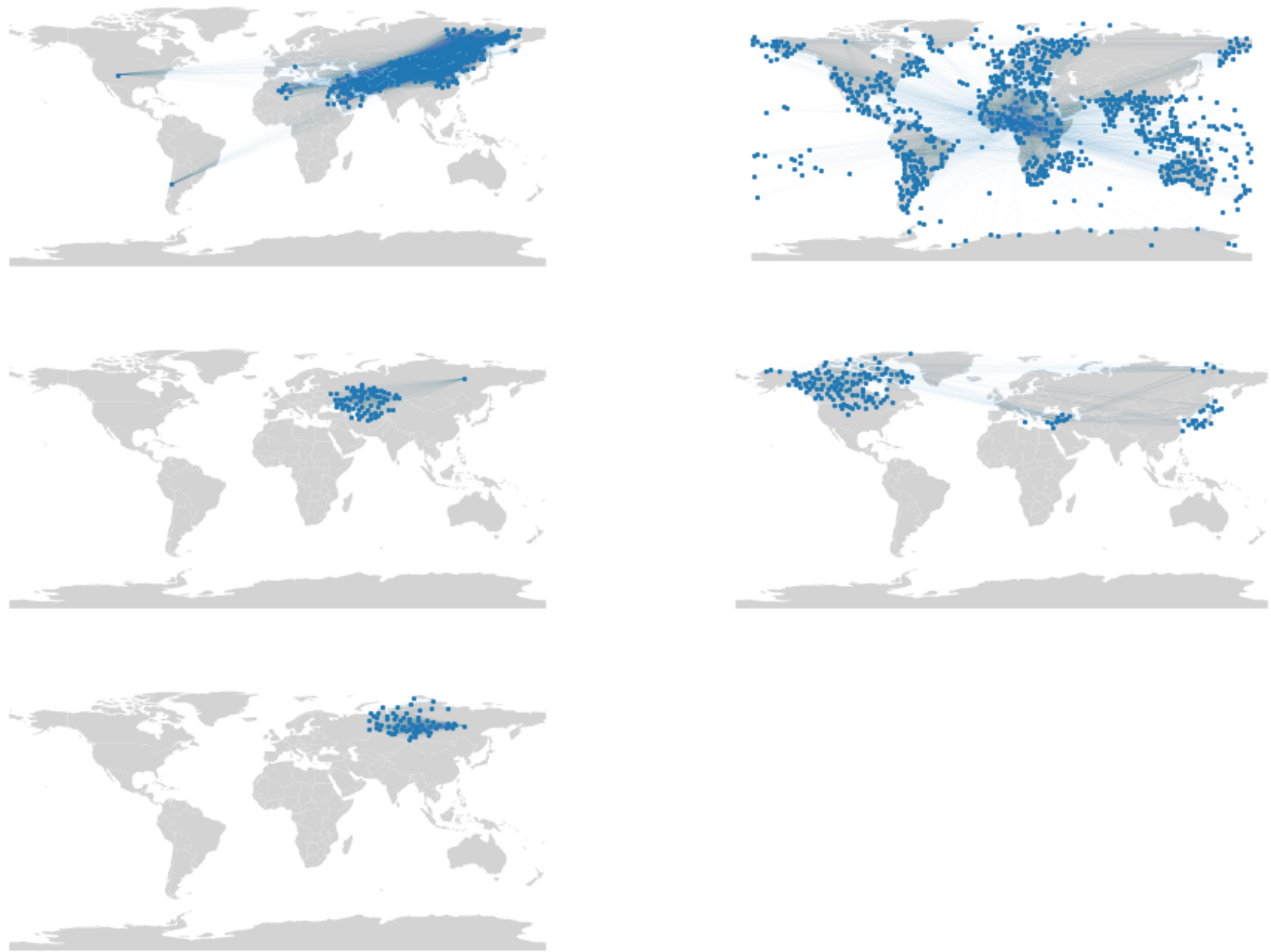


Figure 16. There was a slight decrease in the number of nodes (1%) and edges (12%) in the global climate network of 2000. The average clustering coefficient, on the other hand, increased by 18%. The climate communities discovered were comparable to those detected in the 1990s.

G. Global Climate Network of 2010

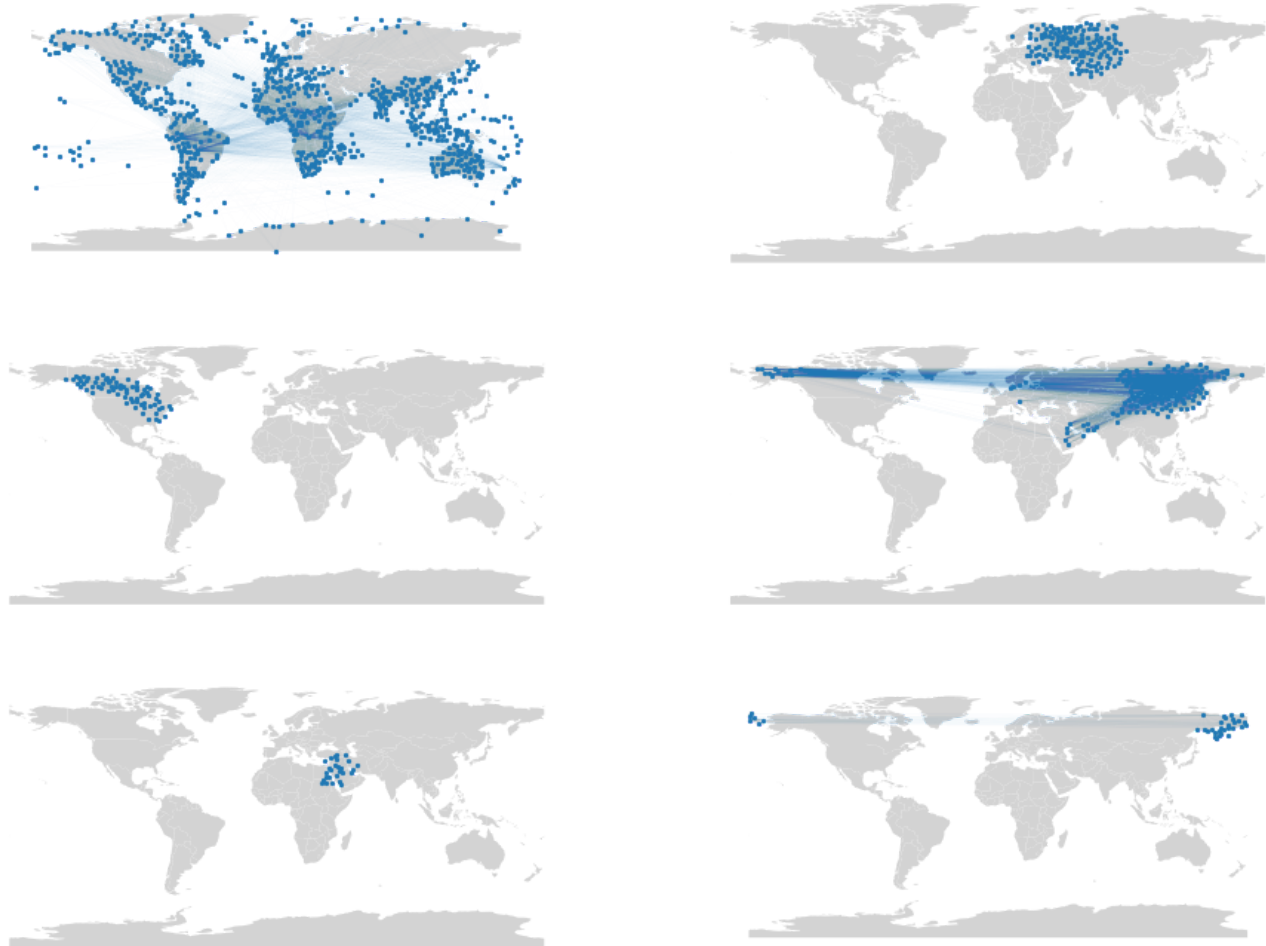


Figure 17. The number of nodes (1,268), the number of edges (21,603), and the average clustering coefficient (0.42) of the global climate network of 2010 are comparable with the 2000 network. The two detected large climate communities, on the other hand, appear to increase in size.